

Spike Onset Dynamics and Response Speed in Neuronal Populations

Wei Wei and Fred Wolf

*MPI for Dynamics and Self-Organization, Faculty of physics, Georg-August University,
and Bernstein center for computational neuroscience, Göttingen, Germany*

Recent studies of cortical neurons driven by fluctuating currents revealed cutoff frequencies for action potential encoding of several hundred Hz. Theoretical studies of biophysical neuron models have predicted a much lower cutoff frequency of the order of average firing rate or the inverse membrane time constant. The biophysical origin of the observed high cutoff frequencies is thus not well understood. Here we introduce a neuron model with dynamical action potential generation, in which the linear response can be analytically calculated for uncorrelated synaptic noise. We find that the cutoff frequencies increase to very large values when the time scale of action potential initiation becomes short.

PACS numbers: 87.19.1l, 05.40.-a, 87.19.ls

Keywords: Action potential, Onset rapidness, Linear response, Cut-off frequency

In the cerebral cortex of the brain information is encoded in the action potential (AP) firing rates of a large ensemble of nerve cells. Recent experiments have observed a surprisingly high cutoff frequency for the action potential encoding of cortical neurons driven by fluctuating input currents [1–4]. In a seminal paper Köndgen *et al.* showed that the transmission function of layer 5 pyramidal neurons for a noisy sinusoidal signal does not decay until about 200 Hz [1]. Later experiments confirmed such high cutoff frequencies for signals coded by both the mean current and noise strength [2] and in other types of cortical neurons [3, 4]. For an early observation of fast response see [5]. Previous theoretical studies of biophysical neuron models, however, predicted cutoff frequencies of the order of the average firing rate or the inverse membrane time constant (below 20 Hz), much lower than the experimentally observed values [6–8]. Thus, the origin of the high cutoff frequencies found in cortical neurons is currently not well understood. Numerical investigation of neuron models with dynamical AP generation, like the exponential integrate-and-fire (EIF) model or the generalized theta neurons, suggested that details of AP generation can influence the dynamical response of neuronal populations [6–9]. What is missing, however, is a transparent understanding of how and when the population cutoff frequency can dissociate from the basic single neuron timescale set by the mean firing rate and the time constant of membrane potential relaxation.

In this work we present an analytically solvable model which explicitly describes the dynamical AP initiation process. A neuron initiates an AP if the membrane potential passes an unstable fixed point, the voltage threshold. In the leaky integrate-and-fire (LIF) model, for which the linear response is known analytically, the unstable fixed point coincides with the absorbing boundary and a spike is triggered immediately when the membrane potential reaches this threshold [10, 11]. As a consequence, boundary induced artifacts dominate the response for high signal frequencies in the LIF model [6–8].

One important advantage of our new model is that such boundary induced artifacts can be separated out mathematically, isolating the physically meaningful part of the response function. We first present the linear response for both encoding paradigms with white noise. We find that for a wide range of parameter settings the cutoff frequency is directly proportional to the AP onset rapidness for a noise coded signal. It therefore dissociates from the membrane time constant and can become arbitrarily large. For the mean current coded signal, however, the cutoff frequency is confined by the membrane time constant in the white noise case. We show by numerical simulation that this confinement can be broken when a finite correlation time in the synaptic noise is taken into account and high cutoff frequencies can be obtained for a large AP onset rapidness. Interestingly, experiments showed that the AP onset rapidness of cortical neurons is very large both *in vitro* and *in vivo* [12, 13], which may thus explain the occurrence of high cutoff frequencies. Our results provide a relationship between the spike onset dynamics and the population cutoff frequency that can be directly tested in physiological experiments.

The simplest voltage dynamics that exhibits both a stable fixed point (the resting potential) and an unstable fixed point (the voltage threshold) has a piecewise linear membrane current, composed of a leak current for low potential and a linear spike generating current for high potential [Fig. 1(a)]. The model is defined by the following Langevin equation

$$\tau_m \dot{v} = -v + \Theta(v - v_0) (r + 1)(v - v_0) + \mu + \sigma \eta(t), \quad (1)$$

where v is the membrane potential relative to the resting potential, τ_m is the membrane time constant, $\Theta(v)$ is the Heaviside step function, r is the AP onset rapidness which sets an effective time constant τ_m/r for the AP initiation process. The larger is r , the faster is the spike onset [Fig. 1(b)]. In biophysical models, the onset rapidness will be set largely by intrinsic properties of the voltage dependent sodium channels, e.g., the gating

charge and the slope of the activation curve [12]. μ is the mean input current and σ is the amplitude of synaptic noise. $\eta(t)$ is a Gaussian white noise satisfying $\langle \eta(t) \rangle = 0$ and $\langle \eta(t)\eta(t') \rangle = \tau_m \delta(t - t')$. The crossing point v_0 of the two pieces sets the rheobase current, which we use as the unit of voltage, $v_0 = 1$. The threshold potential is $v_t = (1 + 1/r)v_0$. When the membrane potential reaches v_b , the truncation point of the AP upstroke, it is reset to a voltage v_r and stays there for an absolute refractory period τ_r . For convenience we take τ_m as the unit of time in analytical calculation.

The Fokker-Plank equation corresponding to Eq. (1) has the following form

$$\begin{aligned} \partial_t P_1 + \partial_v \left(-v + \mu - \frac{1}{2} \sigma^2 \partial_v \right) P_1 &= 0, \\ \partial_t P_2 + \partial_v \left(r(v - v_t) + \mu - \frac{1}{2} \sigma^2 \partial_v \right) P_2 &= 0, \end{aligned} \quad (2)$$

where $P_1(v, t)$ and $P_2(v, t)$ are the probability densities of membrane potential v for $-\infty < v \leq 1$ and $1 < v \leq v_b$ respectively. The stationary firing rate can be found easily when the boundary conditions are specified. From the reset assumption, we impose an absorbing boundary at v_b and, as a result the probability density is zero there, $P_2(v_b, t) = 0$. The firing rate is given by the probability current at v_b , $\nu(t) = -\frac{1}{2} \sigma^2 \partial_v P_2(v_b, t)$. At the reset voltage v_r , the probability density is continuous, while its first derivative has a discontinuity from the reset condition: $\partial_v P_1(v_r^+, t) - \partial_v P_1(v_r^-, t) = \partial_v P_2(v_b, t - \tau_r)$. In addition, the density and its first derivative should be continuous at $v = 1$. When μ and σ are constants, the system is homogeneous and the stationary solution of Eq. (2), denoted as $P_{01}(v)$ and $P_{02}(v)$ respectively, can be found. The stationary firing rate ν_0 is then obtained from the normalization condition of the density [14].

The stationary firing rate ν_0 of the model Eq. (1) reduces to that for the LIF model for $r \rightarrow \infty$. Figure 1(c) and D show the dependence of ν_0 on the mean input μ and the amplitude of noise σ , respectively. The firing rate ν_0 increases monotonically with r , μ , and σ and is relatively insensitive to r when $r > 10$. For the dynamical response, however, the r dependence is much more pronounced. The instantaneous firing rate of an ensemble of model neurons responds much faster for larger r to a step change in the noise level [14].

Linear response.— When the input current to a neuron is weakly modulated, linear response theory can be applied to study the dynamical response properties of an ensemble of neurons. To this end, we consider a sinusoidal signal $\varepsilon \cos(\omega t)$, where ε is small. When the signal is encoded in the mean current, $\mu \rightarrow \mu + \varepsilon \cos(\omega t)$ or in the noise amplitude, $\sigma \rightarrow \sigma + \varepsilon \cos(\omega t)$, the instantaneous firing rate can be written as $\nu(t) = \nu_0 + \varepsilon |\nu_{1c}(\omega)| \cos(\omega t - \phi_c(\omega))$ or $\nu(t) = \nu_0 + \varepsilon \sigma |\nu_{1n}(\omega)| \cos(\omega t - \phi_n(\omega))$. Here $\nu_1(\omega)$ are the complex response functions. The absolute

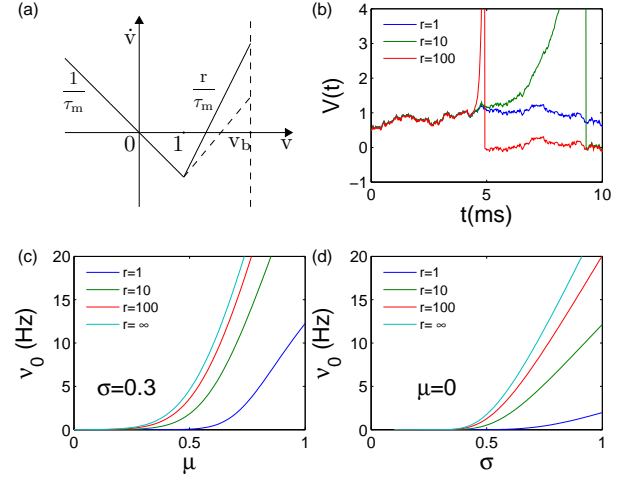


FIG. 1: (color online) (a) Illustration of the model. (b) $V(t)$ trajectories for identical noise and three different values of r . (c) and (d) show the dependence of stationary firing rate on mean input current and noise strength in the noise driven regime. ($\tau_m = 10$ ms, $v_r = 0$, $v_b = 10$, $\tau_r = 0$)

value $|\nu_1(\omega)|$ are the transmission functions and the phase angles $\phi_1(\omega) = \arg(\nu_1(\omega))$ give the phase lags, which completely characterize the linear response. Note that we refer to both signal channels when the subscripts c and n are omitted.

It is known that the absorbing boundary condition at v_b can induce severe artifacts in the dynamical response. The potential v_b marks a "point of no return," which is not present in a biophysical dynamical model of AP initiation. As a consequence, the transmission function for a noise coded signal in the LIF model, for instance, does not decay at high signal frequencies [5, 11]. Ideally one would thus wish to separate the response function into a physiologically meaningful part $\nu_1^{phy}(\omega)$ and a part containing all artifacts such that $\nu_1^{phy}(\omega) = \nu_1(\omega) - \nu_1^{abs}(\omega)$. $\nu_1^{phy}(\omega)$ must have the following properties: i) $\nu_1^{phy}(\omega)$ approaches the static susceptibility when $\omega \rightarrow 0$, specifically, $\nu_{1c}^{phy}(\omega) \rightarrow \frac{\partial \nu_0}{\partial \mu}$ and $\nu_{1n}^{phy}(\omega) \rightarrow \frac{1}{\sigma} \frac{\partial \nu_0}{\partial \sigma}$; ii) $\nu_1^{phy}(\omega) \rightarrow 0$ when $\omega \rightarrow \infty$; iii) no essential dependence on the truncation point v_b . The artifactual part from the absorbing boundary should have the following properties: i) negligible contribution for signal frequency in the physiologically relevant range $f \leq 1$ kHz, e.g. $|\nu_1^{abs}(\omega)| \ll |\nu_1^{phy}(\omega)|$, where $f = \omega/2\pi$; ii) strong dependence on the truncation point v_b . As we will show next such an isolation of the physiologically meaningful response is possible in the model Eq. (1).

In the model Eq. (1), the linear response can be obtained analytically by expanding the probability density in Eq. (2) to first order in ε and using the Green's function method. We find that $\nu_{1n}(\omega)$ decomposes naturally into two parts, $\nu_1(\omega) = \nu_1^{Low}(\omega) + \nu_1^{High}(\omega)$, with

$$\begin{aligned}\nu_{1c}^{Low}(\omega) &= \frac{i\omega}{(1-i\omega)(1+i\omega/r)} \frac{(1+1/r)(\psi_1 P_{01} - \sqrt{D}\Phi_1 P'_{01}) - (1+i\omega/r)\Phi_1(v_r)e^{\Delta_0+i\omega\tau_r}}{\psi_1(v_r)e^{\Delta_0+i\omega\tau_r} + (Y_1\psi'_1 - Y'_1\psi_1)e^{\Delta_1}}, \\ \nu_{1n}^{Low}(\omega) &= \frac{i\omega(i\omega-1)}{(2-i\omega)(2+i\omega/r)} \frac{(1+1/r)\left(\frac{i\omega}{(1-i\omega)\sqrt{D}}\Phi_1 P_{01} + 2Y_1 P'_{01}\right) + \frac{\nu_0}{D}(2+i\omega/r)\Upsilon(v_r)e^{\Delta_0+i\omega\tau_r}}{\psi_1(v_r)e^{\Delta_0+i\omega\tau_r} + (Y_1\psi'_1 - Y'_1\psi_1)e^{\Delta_1}},\end{aligned}\quad (3)$$

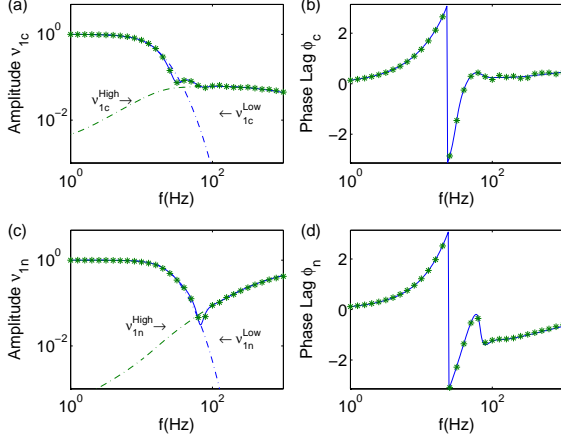


FIG. 2: (color online) The normalized function $\nu_1(\omega)/\nu_1(0.1)$ and phase lag for a mean coded signal and noise coded signal with $r = 1$, $\mu = 0$, and $\nu_0 = 5$ Hz. Other parameters are the same as in Fig. 1. Lines, theory; Symbols, simulation.

where $D = \frac{1}{2}\sigma^2$, $\Delta_0 = (1 - v_r)(2\mu - 1 - v_r)/4D$ and $\Delta_1 = (1 - v_b)(2\mu - 1 + r(v_b - v_t))/4D$. ψ_1 , Φ_1 , and Υ_1 are parabolic cylinder functions, and Y_1 , Y_2 are a combination of parabolic cylinder functions, whose definition together with the $\nu_1^{High}(\omega)$ parts are given in the supplement [14]. Any prime represents the derivative with respect to v . Here and in the following, the functions adopt their values at $v = 1$ if not denoted explicitly. Figure 2 illustrates the linear response with $r = 1$ as an example.

Removing boundary induced artifacts.— The decomposition of $\nu_1(\omega)$ into two additive components has exactly the features required for the separation of artifacts. Using asymptotic expansion of the parabolic cylinder functions we find that for a finite signal frequency, ν_1^{High} can be approximated by

$$\begin{aligned}\nu_{1c}^{High}(\omega) &\simeq \frac{\nu_0}{r(v_b - v_t) + \mu} \frac{i\omega}{r + i\omega}, \\ \nu_{1n}^{High}(\omega) &\simeq -\frac{\nu_0}{(r(v_b - v_t) + \mu)^2} \frac{i\omega(1 + i\omega/r)}{2 + i\omega/r}.\end{aligned}\quad (4)$$

when $v_b \gg v_t$. So $\nu_1^{High}(\omega)$ are strongly dependent on v_b and approach zero when $v_b \rightarrow \infty$ for finite signal frequency. When $\omega \rightarrow 0$, $\nu_1^{High}(\omega)$ are negligible compared with $\nu_1^{Low}(\omega)$ and are strongly suppressed when v_b is large. That $\nu_{1n}^{High}(\omega)$ captures all artificial con-

tributions imposed by the absorbing boundary condition is finally confirmed from the high frequency behavior, $\nu_{1c}^{High}(\omega) \rightarrow \frac{\nu_0}{\sqrt{D}} \frac{1}{\sqrt{\omega}} e^{i\pi/4} = \lim_{\omega \rightarrow \infty} \nu_{1c}^{LIF}(\omega)$ and $\nu_{1n}^{High}(\omega) \rightarrow \frac{\nu_0}{D} = \lim_{\omega \rightarrow \infty} \nu_{1n}^{LIF}(\omega)$, since the high frequency behavior in the LIF model is determined solely by the absorbing boundary. As a consequence, neglecting $\nu_{1n}^{High}(\omega)$ in the response function eliminates any boundary induced instantaneous response components. These results establish that $\nu_1^{Low}(\omega)$ capture the behavior of $\nu_1(\omega)$ for low and intermediate frequencies and decay to zero in the large frequency limit. When $\omega \rightarrow 0$, $\nu_{1n}^{Low}(\omega) \rightarrow \nu_{1n}(0) = \frac{1}{\sigma} \frac{\partial \nu_0}{\partial \sigma}$, since $\nu_{1n}^{High}(\omega)$ is negligible there. $\nu_1^{Low}(\omega)$ exhibits only a weak dependence on v_b through a frequency dependence phase lag $\phi_0 = \frac{\omega}{r} \log \frac{v_b + \mu}{\sqrt{rD}}$, characterizing the time lag to the truncation point v_b of the AP upstroke. Therefore, we have $\nu_1^{Low}(\omega) = \nu_1^{phy}(\omega)$. The physiologically meaningful predictions of the model can thus be revealed by examining $\nu_1^{Low}(\omega)$ in isolation.

Cutoff frequency and AP onset rapidness.— Figure 3 shows the behavior of $\nu_1^{Low}(\omega)$ with increasing r and how the cutoff frequency f_c changes with r for different ν_0 [15]. We see that f_c increases linearly with the onset rapidness r for noise coded signals when the firing rate is not very low (> 1 Hz here); while for mean coded signals f_c saturate for large r . The increase of f_c with firing rate ν_0 results from the stochastic double resonance phenomenon: the transmission function will develop a peak for some optimal signal frequency before decaying when ν_0 is relatively large [16].

Figure 3D suggests that the cutoff frequency for a noise coded signal follows $f_c \propto r$ and dissociates from τ_m . This is directly confirmed by the large frequency approximation of $\nu_{1n}^{Low}(\omega)$,

$$\nu_{1n}^{Low}(\omega) \propto \frac{\exp(-\frac{\pi}{4}\omega/r)}{2 + i\omega/r} \left(-P'_{01} + \frac{i\sqrt{i\omega/r}}{2\sqrt{D}} \tilde{P}_{01} \right), \quad (5)$$

where $\tilde{P}_{01}(v) \equiv \sqrt{r}P_{01}(v)$. Because $\tilde{P}_{01}(v_0) \rightarrow \sqrt{\frac{\pi}{2}} \frac{\nu_0}{\sqrt{D}}$ and $P'_{01}(v_0) \rightarrow -\frac{\nu_0}{D}$ for $r \gg 1$, the decay of $\nu_{1n}^{Low}(\omega)$ depends essentially only on ω/r . This implies that the cutoff frequency for a noise coded signal dissociates from τ_m and becomes proportional to the onset rapidness r , $f_c = Ar$, where A depends on ν_0 through the effect discussed above. This demonstrates that fast onset APs can enhance the cutoff frequency and therefore the response speed significantly. Note that a linear relationship $f_c \propto r$

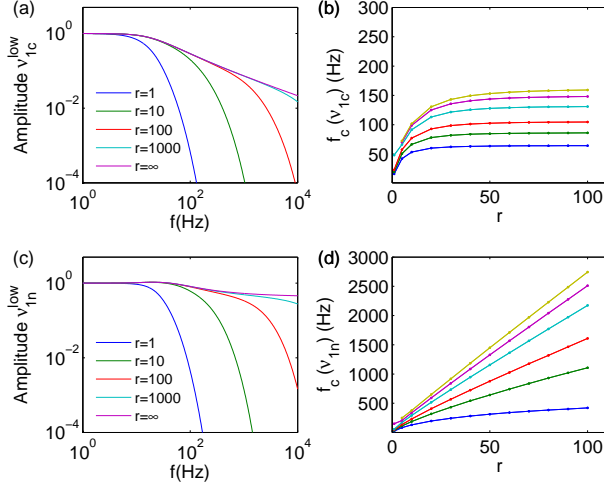


FIG. 3: (color online) (a) and (c) The normalized transmission function $\nu_{1c}^{low}(\omega)/\nu_1(0.1)$ for different r with $\mu = 0$, $\nu_0 = 5$ Hz. (b) and (d) The variation of cutoff frequency with r for different firing rates: $\nu_0 = 1, 5, 10, 20, 30, 40$ Hz from lower to upper curves. Other parameters are the same as in Fig. 1.

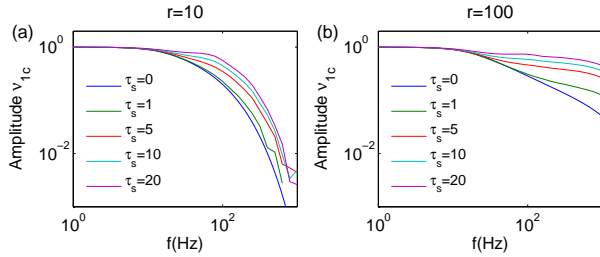


FIG. 4: Variation of the normalized transmission function $|\nu_{1c}(\omega)/\nu_{1c}(0.1)|$ with increasing correlation time τ_s (with unit ms) of the synaptic noise for $r = 10, 100$. Parameter used: $\mu = 0$, $v_b = 10$, $\nu_0 = 5$ Hz.

was previously conjectured by Naundorf *et al.* based on dimensional analysis [18].

For a current coded signal, however, $\nu_{1c}^{low}(\omega) \propto \frac{1}{\sqrt{\omega}} \exp(-\frac{\pi}{4}\omega/r)$ for large r . Therefore the linear response is confined by the membrane time constant in the white noise case, as seen also from Fig. 3A. Real synaptic inputs, however, have a finite correlation time and can be approximated better as a colored noise. As shown in Fig. 4, the confinement by the membrane time constant is broken under such conditions and cutoff frequencies of several hundred Hz can be reached for large r [14].

Our results identify AP onset rapidness as a critical determinant of population cutoff frequency and reveal how this cutoff frequency can dissociate from the basic single neuron time constants set by the mean firing rate and

membrane time constant. The confinement of the mean response for white noise constitutes an interesting prediction of the model, which should be tested experimentally by using a very short correlation time (≤ 1 ms) of the synaptic noise. The origin of the large onset rapidness seen in cortical neurons is a matter of ongoing debate [17, 18]. Its value can be modified in real neurons by applying drugs like TTX or knockout of sodium channel subtypes [12, 19]. Measurements of dynamical response for cortical neurons under such manipulations are thus predicted to provide important insight into the mechanism of fast population coding.

We thank D. Battaglia and B. Lindner for suggestions and carefully reading an early version of the manuscript. We are grateful to T. Geisel, M. Gutnick, M. Huang, M. Monteforte, T. Moser and T. Tchumatchenko for discussions. This work was supported by BMBF (01GQ07113), GIF (906-17.1/2006), BCCN II (01GQ1005B), and DFG (SFD899).

-
- [1] H. Köndgen *et al.*, Cereb. Cortex **18**, 2086 (2008).
 - [2] C. Bucci *et al.*, J. Neurosci. **29**, 1006 (2009).
 - [3] M. Higgs, W. Spain, J. Neurosci. **29**, 1285 (2009).
 - [4] T. Tchumatchenko *et al.*, to be published.
 - [5] G. Silberberg *et al.*, J. Neurophysiol. **91**, 704 (2004).
 - [6] N. Fourcaud-Trocmé *et al.*, J. Neurosci. **23**, 11628 (2003).
 - [7] N. Fourcaud-Trocmé, N. Brunel, J. Comput. Neurosci. **18**, 311 (2005).
 - [8] B. Naundorf, T. Geisel, F. Wolf, J. Comput. Neurosci. **18**, 297 (2005).
 - [9] M. Richardson, Phys. Rev. E **76**, 021919 (2007).
 - [10] N. Brunel *et al.*, Phys Rev Lett **86**, 2186 (2001).
 - [11] B. Lindner, L. Schimansky-Geier, Phys Rev Lett **86**, 2934 (2001).
 - [12] B. Naundorf, F. Wolf, M. Volgushev, Nature **440**, 1060 (2006).
 - [13] L. Badel *et al.*, J. Neurophysiol. **99**, 656 (2008).
 - [14] See supplemental material at <http://link.aps.org/supplemental/10.1103/PhysRevLett.106.088102>.
 - [15] For LIF model, $|\nu_{1n}(\omega)|$ starts at zero signal frequency with a value $\frac{\partial \nu_0}{\partial D}$ and saturates to a constant $\frac{\nu_0}{D}$ at large frequency. So in our model there will be a transition between these two plateaus before the decaying of transmission function, since in large r limit it reduces to the LIF model. To characterize the decaying property and avoid the transition region, we extract the cut-off frequencies at which the normalized transmission function decays to $1/\sqrt{10}$, which is smaller than the value usually adopted.
 - [16] H. Plesser and T. Geisel, Phys. Rev. E **59**, 7008 (1999).
 - [17] D. McCormick, Y. Shu, Y. Yu, Nature **445**:E1-E2(2007).
 - [18] B. Naundorf, F. Wolf, M. Volgushev, Nature **445**:E2-E3 (2007).
 - [19] M. Royeck *et al.*, J. Neurophysiol. **100**, 2361 (2008).